H1-06/00-586

ET-8 Tagger Performance and User Guide.

V.Andreev, A.Fomenko, E.Malinovski, I.Sheviakov and Yu.Soloviev

P.N.Lebedev Physical Institute, Moscow, Russia

Abstract

The H1 detector at HERA has been upgraded by the addition of a new electromagnetic calorimeter. It has been installed in the HERA tunnel close to the e-beam line at a position $\simeq 8$ m from the interaction point in the electron beam direction. The new calorimeter allows to extend the present acceptance for tagged photoproduction events to the high y range, $0.80 < y < 0.95$, and thus significantly improves the capability of H1 to study γp processes. The calorimeter design, performance, acceptance determination and obtained results using this calorimeter during 1998-1999 HERA Luminosity Runs are described.

1 Introduction

The electron calorimeter ET-8 was installed in the HERA tunnel in 1998 at the distance 8 m from the interaction point. The existing electron detectors ET-33 and ET-44 tagg the quasi-real ($Q^2 \sim 0$) photons in the energy range $0.3 \leq E_\gamma/E_e \leq 0.8$ and $0.08 \leq E_\gamma/E_e \leq 0.20$, where the energy E'_e in these calorimeters is related to the photon energy E_γ by:

$$y = 1 - E'_e/E_e \ \sin^2\theta/2 = 1 - E'_e/E_e + Q^2/E^2 \simeq 1 - E'_e/E_e = E_\gamma/E_e.$$

The new electron tagger is efficiently detects the scattered electrons with the energy of several GeV that allows the photoproduction processes with the higher photon energy $W_{\gamma p} \simeq 300\ GeV$ to be tagged.

Fig.1 shows the calculated acceptances of the different electron calorimeters (ET-33, ET-44 and ET-8) for the photoproduction process with the nominal beam conditions (zero tilt and offset). One can see that the proposed electron tagger ET-8 extends the measurable y-range to the high y interval $0.80 < y < 0.95$.

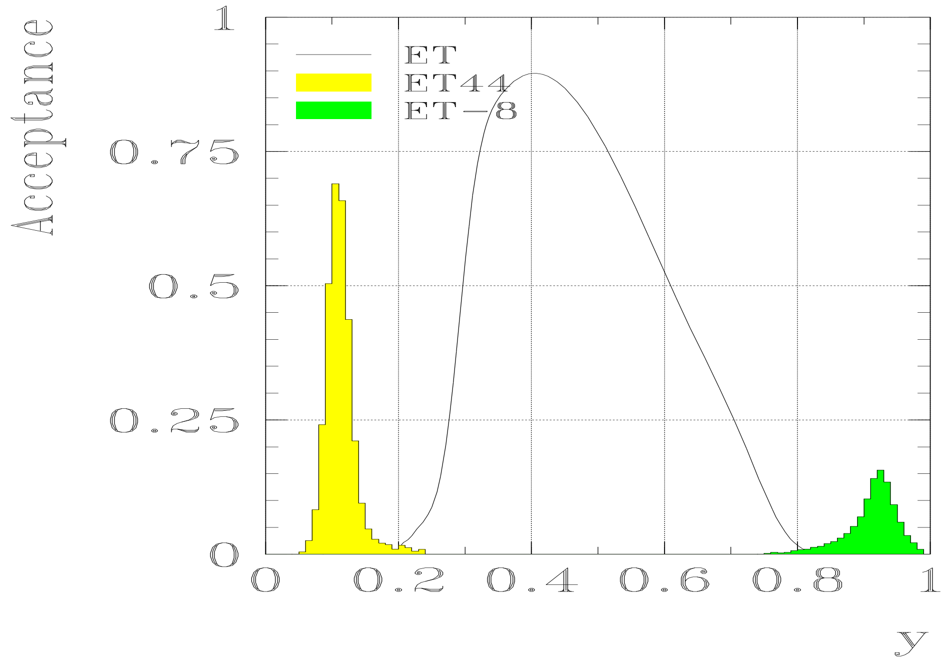

Figure 1: Acceptances of the three electron taggers for photoproduction with nominal e-beam conditions.

2 Detector design

In contrast to other luminosity calorimeters (using the Čherenkov KRS and NBW crystals as radiator) the new electron tagger is a spaghetti type calorimeter. It is built up from SpaCal modules which form the present SpaCal calorimeter in H1 [1] .

The schematic view of the ET-8 fiber detector, its granularity and coupling principle are drawn in Fig.2. The total longitudinal dimension of the active calorimeter volume which has to contain the showers is 92 mm.

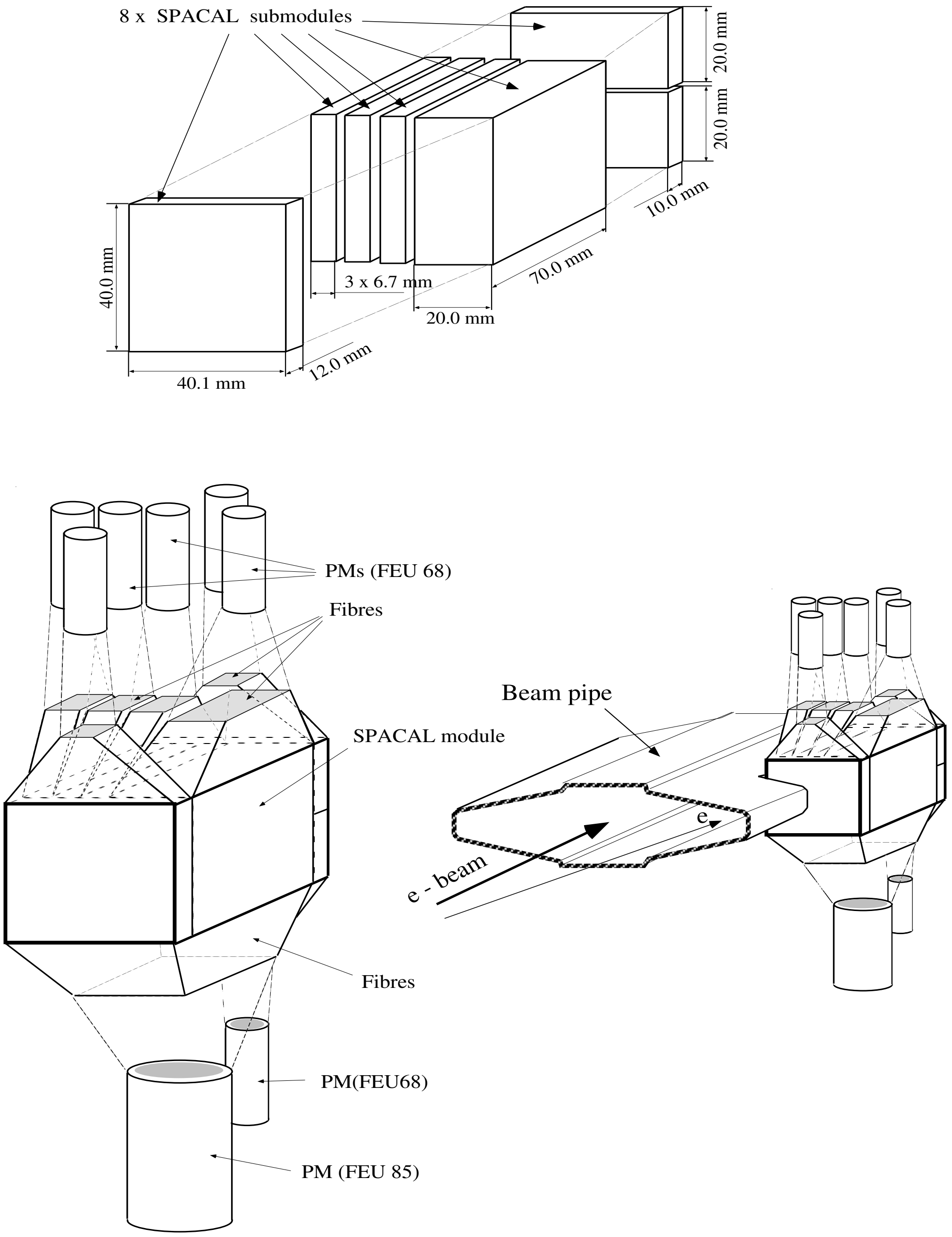

Figure 2: Design and installation of ET-8 calorimeter in the HERA tunnel

The calorimeter consists of three parts: the front tagging counter made as a SpaCal plate of 1.2 X_o thickness, a central part and a back coordinate plane. The central part with cross section of 40x40 cm^2 and 70 mm length corresponding to 9 X_o consists of 4 blocks. As the main part of the accepted events have the point of electron incidence near the boundary close to the electron beam the 3 leftmost blocks have the width of 6.7 mm. It allows the horizontal hit point coordinate to be determinated exploiting the sharing of energies between submodules of the central part. The vertical coordinate is determinated from the ratio of output responses of the upper and lower submodules placed in the rear end of ET-8 calorimeter. To avoid the directional confusion in the measuring scattered electrons the signal from the front tagging plate is required in coincidence with the energy deposited in the central part. Thus it is possible to veto events not entering via the detector front plane.

The Level 1 trigger element for the new electron tagger requires a simple condition $E_{dep}^{tot} > E_{thr}$, where E_{dep}^{tot} is the total deposited energy in the calorimeter and E_{thr} the threshold energy which must have a low value, $E_{thr} \simeq 0.5 - 1.0$ GeV. A minimum ionizating particle deposits only 50 MeV. An additional γ-veto condition from the photon arm of the luminosity system (no signal in Photon Detector) suppresses the high background from the Bethe-Heitler process $ep \to e\gamma p$ [2] with an efficiency $\sim 95 - 98$ %.

3 Experimental data

3.1 Rate and event selection

The new electron detector started measuring in the second half of 1998. The Fig. 3 shows the contribution of different sources to the total rate in ET-8 during one luminosity run.

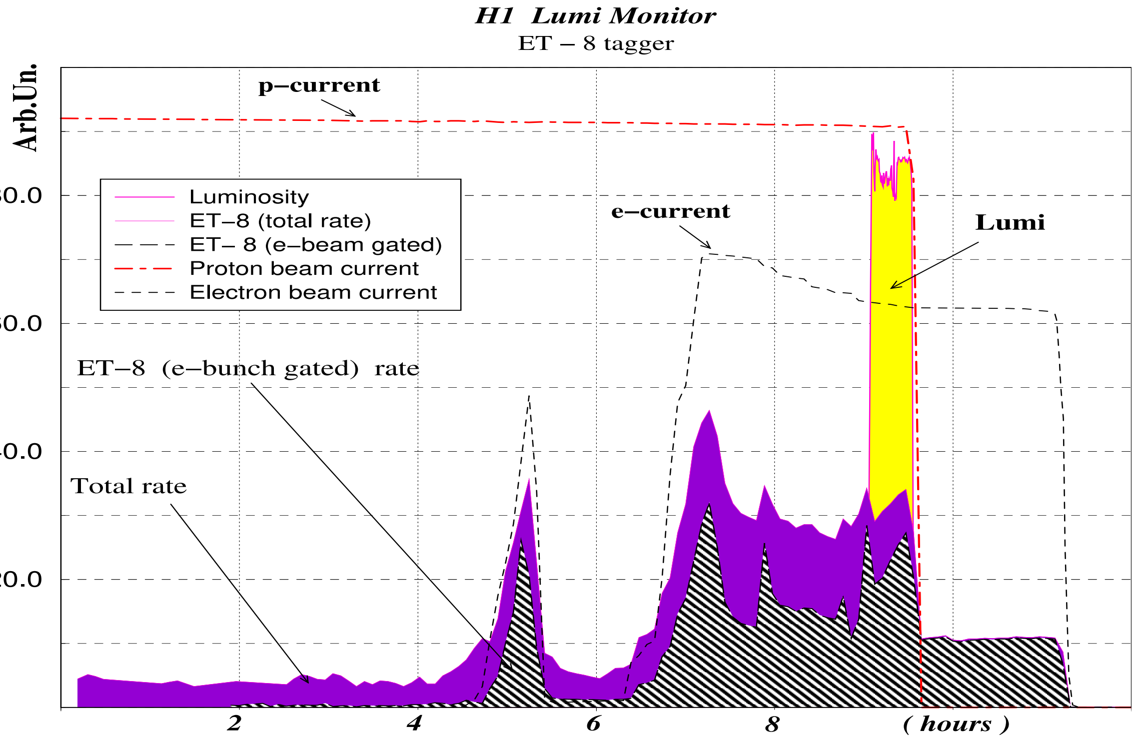

Figure 3: The components of the ET-8 calorimeter rate as function of the time during the luminosity run.

During the first 2 hours there was only stable 920 GeV p-beam and the ET-8 total rate was only produced by p-beam halo particles hitting the detector. After injection and keeping of low current 12 GeV electron beam between 2^{nd} and 5^{th} hour a significant part of electrons were lost under an attempt to inject a high current of electrons. At the 7^{th} hour a high current 12 GeV electron beam was successfully injected and ramped up to 27.6 GeV. During this period the ET-8 rate apart from a p-beam induced component includes one depending on e-beam presence in HERA: scattered electrons from bremsstrahlung events at residual gas at HERA beam pipe and so-called "$off-momentum$" electrons. Lumi conditions were achieved at the 9^{th} hour and soon afterwards the p-beam was lost while the electron beam was kept at HERA up to 11^{th} hour. If the final phase of the rate plot consists of the e-beam induced part only then the Lumi condition ET-8 rate is the most interesting response - it includes all possible components. There is a clear evidence on growing of e-beam gated rate and maintaining of the same level p-beam induced part of the ET-8 rate.

The separation of different background sources that have an influence on the ET-8 tagger rate is the task of the *"H1 Lumi trigger system"*. The averaged FADC pulse shape of the ET-8 response for the events triggered by S99 *"ET-8"* subtrigger is shown in Fig.4. The two spikes represent both: proton halo (first) events and electrons induced events. The histogram corresponds to ET-8 response without any restriction - **a**, and response under conditions where a limited size *"electron window-time"* is used - **b**.

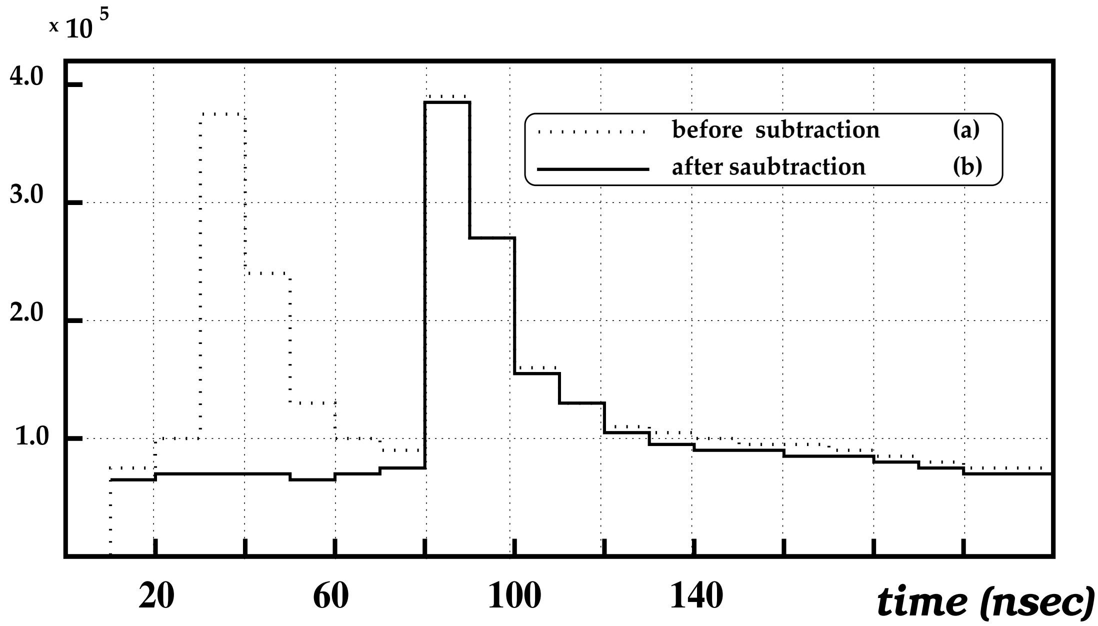

Figure 4: The averaged FADC's pulse shape for the events triggered by *H1 - ET-8* subtrigger: **a** - with proton halo and **b** - after subtraction proton halo.

In order to produce the level one trigger output for the ET-8 detector the data are taken with two independent conditions. The first trigger cut termed above *"electron window-time"* is formed by the coincidence of a response from the ET-8 tagger with a signal coming within the time interval expected for *ep*-interactions. The second trigger cut, termed *"threshold cut'*, requires the simple condition that the energy in the ET-8 detector to be more than E_{thr}. This value was chosen to be $E_{thr} \simeq 1.0\ GeV$.

The correlations between the rates of the different taggers within the one electron fill (one luminosity run) are presented on Fig.5. The relation of the observed rates in the various taggers are in good agreement with the Monte Carlo simulation of bremsstrahlung events taking into account the acceptance of the different taggers. Sudden increase of the ET-44 rate indicates the moment the detector was moved to his working position close to the e-beam axis.

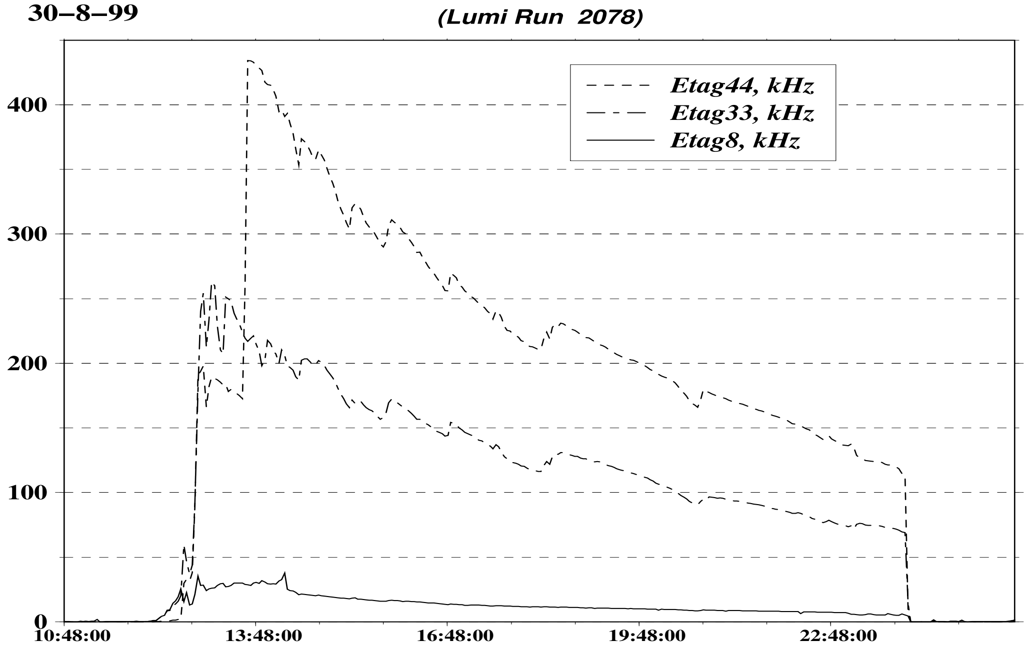

Figure 5: The long term behaviour of the taggers rates within one beam fill.

3.2 Detector calibration

For the calibration of the ET-8 calorimeter and also for the all detectors forming the Luminosity system the Bethe-Heitler bremsstrahlung process $ep \longrightarrow e\gamma p$ is used. Since the energy transfer to the proton is negligible, the relation

$$E_{tagger} + E_\gamma = E_o,$$

where E_o - the electron beam energy, must hold.

The standard calibration procedure described in detail [3] determines the calibration coefficients $C(n)$ by minimizing the following sum:

$$\sum_i \Big(\sum_{n=1}^{N} C(n) * A_i(n) - E_o \Big)^2,$$

where n-is channel number in the detector, N is total number of channels, i-event number, A_i(n)-amplitude of n-th element in i-th event and C(n)-calibration coefficient for n-th element.

The first step of the calibration is based on the fact that the Photon Detector (PD) had been already calibrated together with the main Electron Tagger (ET) inside the Lumi system. In addition the absolute energy scale of the photon detector can be determined using the high energy edge of the bremsstrahlung spectrum [4].

The next step of the calibration is to select the events with an impact point in the front plane of the ET-8 well separated from the detector edges. The distribution of the electron hit points in the ET-8 is shown in Fig.6(a). The nearest to the beam-pipe edge of the detector and an electron exit window is corresponded to the reconstructed coordinate $X_{rec} \simeq$ -2.0 cm. As the size of the exit window is $\sim$ 2 cm the electrons having the x-coordinate $X_{rec} > 0.0$ cm are partially lost its energy in the beam-pipe wall. These events are taken out from the calibration. The using events with $X_{rec} >$ -1.5 cm is connected with the fact that there is a big energy leakage for the electrons with the hit point close to the detector boundary and the energy reconstruction for these events is poor.

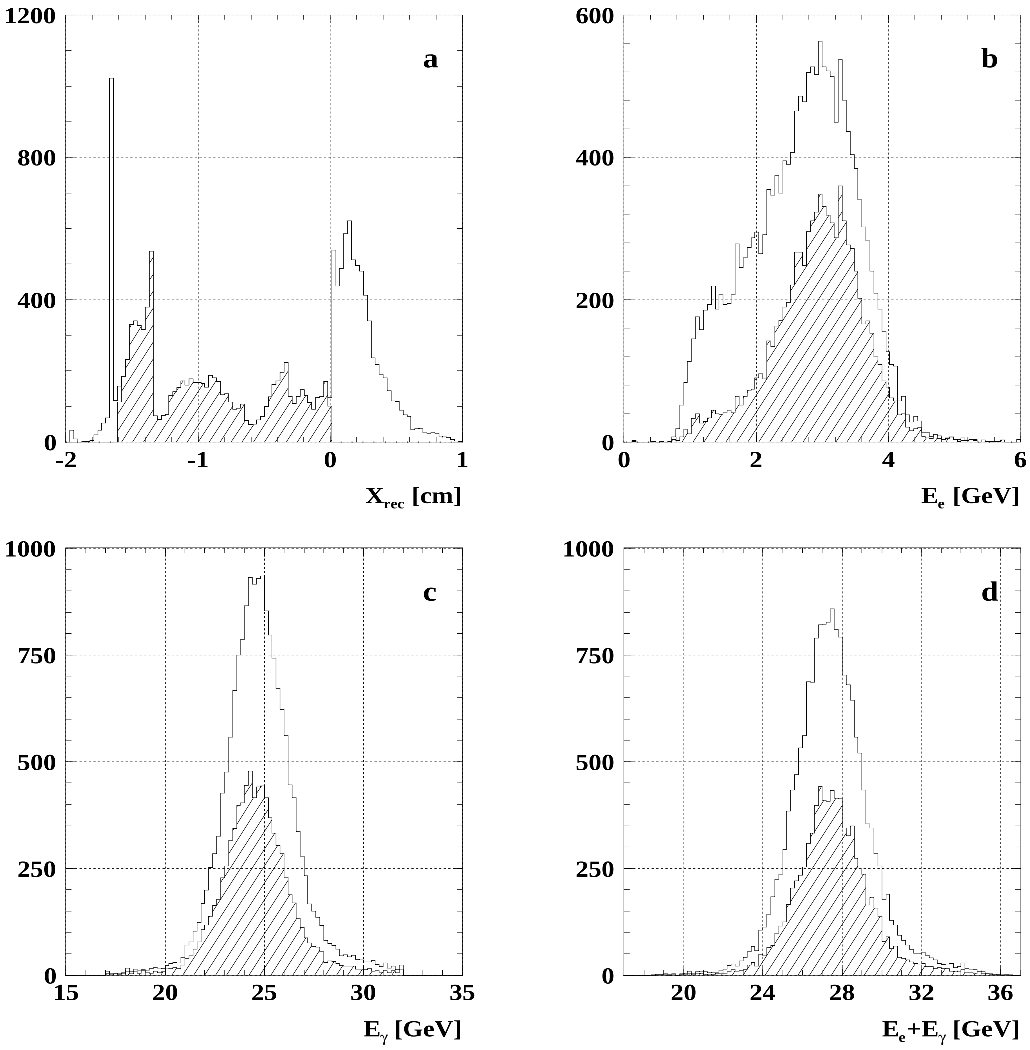

Figure 6: a - reconstruction of the electron hit points in the ET-8; b - energy distribution of the accepted electrons; c - energy distribution of the photons in PD in coincidence with an electron in ET-8; d - sum of the reconstructed photon and electron energies for BH events. Hatched histograms represent the distributions of the events used for the calibration.

Then calibration coefficients for the photon calorimeter are fixed by the joint PD - ET calibration and the individual coefficients for the ET-8 channels are determined from the dedicated run data sample with the ET-8 trigger element. The event selection and the result of the calibration procedure are illustrated in Fig.6.

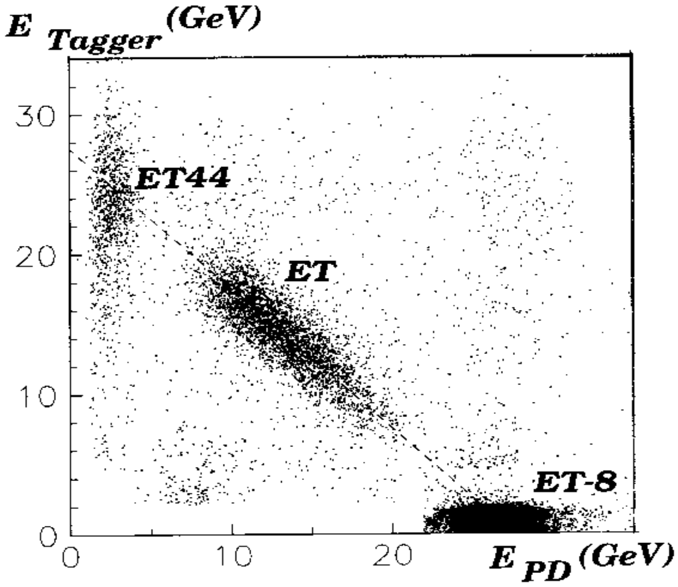

Figure 7: The E_γ - E_e correlation for bremsstrahlung events detected by the H1 luminosity system including all electron taggers: ET, ET44 and ET-8.

Fig.7 shows the correlation between the reconstructed electron E_e and photon E_γ energies for bremsstrahlung events. These samples are selected by the trigger: $ET * PD$, where ET is anyone of ET, ET44 or ET-8, and E_γ=E_{PD}+ E_{VC}. Due to the large difference in trigger rates of different taggers (ET44 $\simeq$ 280 kHz, ET $\simeq$ 170 kHz and ET-8 $\simeq$ 15 kHz at luminosity L = $5 * 10^{30}$ $cm^{-2}s^{-1}$) these data have been taken with various prescale conditions for their trigger elements. Here it is necessary to emphasize that corresponding distribution of $E_e + E_\gamma$ for every taggers is well described by Gaussian function with mean value of 27.6 GeV and the standard deviation of $\simeq$ 1.5 GeV.

3.3 Trigger efficiency

The important characteristic of the detector is a behaviour of the trigger threshold and its efficiency. Usually these values are determinated using a random sample. In our case the *"pseudo-random S91-subtrigger"* sample was used for this purpose in order to increase statistic. The *"S91-subtrigger"* is formed by the Level 1 **LU_PD_low** trigger element, where **LU_PD_low** requires that the deposited energy in the Photon Detector to be more than the threshold energy $\sim$ 5 GeV.

The energy distributions of the accepted by ET-8 electrons are shown in Fig.8a. The open histogram in this picture contains the events taken by the random trigger and the hatched histogram represents the energy distribution for events in which ET-8 trigger element was set. The maximum around $\sim$ 3.0 GeV corresponds the bremsstrahlung events. Comparing these two histograms one determines the ET-8 trigger efficiency as a function of the electron energy. This dependence is shown in Fig.8b.

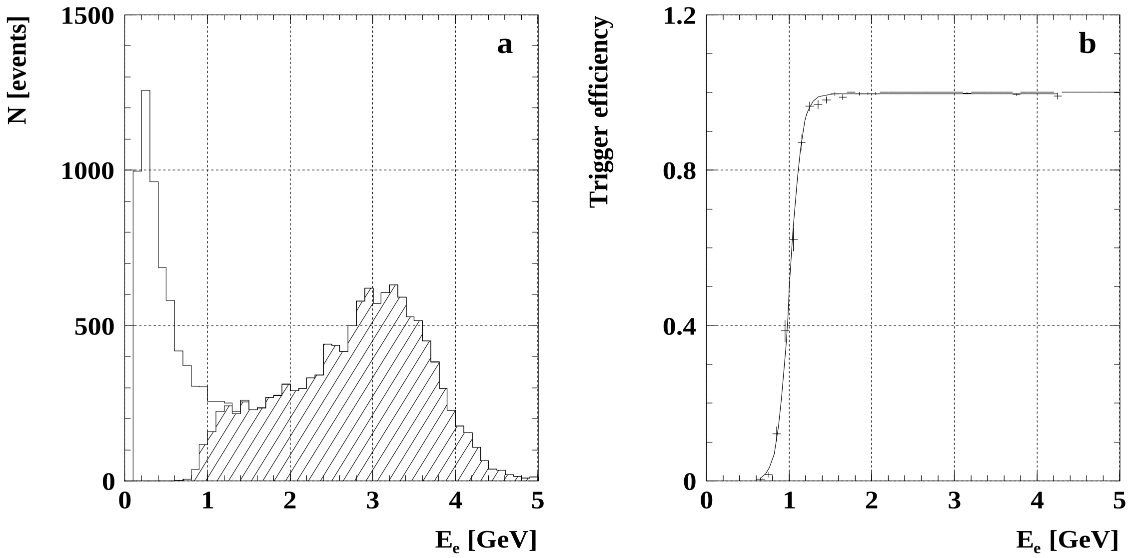

Figure 8: Energy distributions of the accepted electrons: a - assuming *"Level one trigger ET-8"*(hatched histogram) and for *"Random trigger sample"*(open histogram); b - trigger efficiency of ET-8 tagger as a function of electron energy.

The trigger threshold equals $\sim$1.0 GeV for almost all calibration samples but the maximum level of the trigger efficiency is less than 1.0 for some samples (it is varied from $\sim$ 0.5 up to $\sim$ 1.0). The last property is mainly connected with the hardware problems for the separate run periods. The trigger efficiency function is taken into account at the acceptance determination.

4 Acceptance Determination

The acceptance study of the ET-8 as well as others electron calorimeters has been performed using the fast simulation package H1LUMI [5]. This models the current HERA electron ring optics (the proposed spin rotators have yet to be included) as is described in e.g. [6] . One example of such calculation for all 3 electron taggers is shown in Fig.1 . Small possible variations of the beam parameters at the IP (horizontal θ_x, vertical θ_y tilt of $\pm$0.15 mrad and offsets X_{off}, Y_{off} $\pm 1mm$) have been taken into account in the simulation. They typically lead to 15-25 % changes in the electron tagger acceptance. In order to reduce this kind of uncertainty the acceptance was derived from data using $ep \rightarrow e\gamma p$ events. This allows the acceptance to be determinated with necessary precision. This procedure has been used for the ET-33 [7] and ET-44 [8] electron calorimeters before.

The horizontal θ_x and vertical θ_y tilts of the electron beam in the interaction point are the electron beam parameters which influence the acceptance These parameters are measured from the distribution of the photons hit point in the Photon Detector for the BH events.

The next two important parameters are X_{off}, Y_{off} - horizontal and vertical offset of the electron beam. To first order the acceptance dependence on the vertical offset Y_{off} is negligible and will not be taken into account. The X_{off} value is determined from the tuning MC (H1LUMI package) by changing the electron trajectory offset as input parameter such way that the best description of the data is obtained. The example of such procedure for the 2 data sample in 1999 is given in Fig.9 and Fig.10.

Fig.9 presents data collected in the first half of 1999 when HERA operated with the electron beam. One can see that the trigger efficiency threshold plays an important role in this case and it is also taken into account in the tuning.

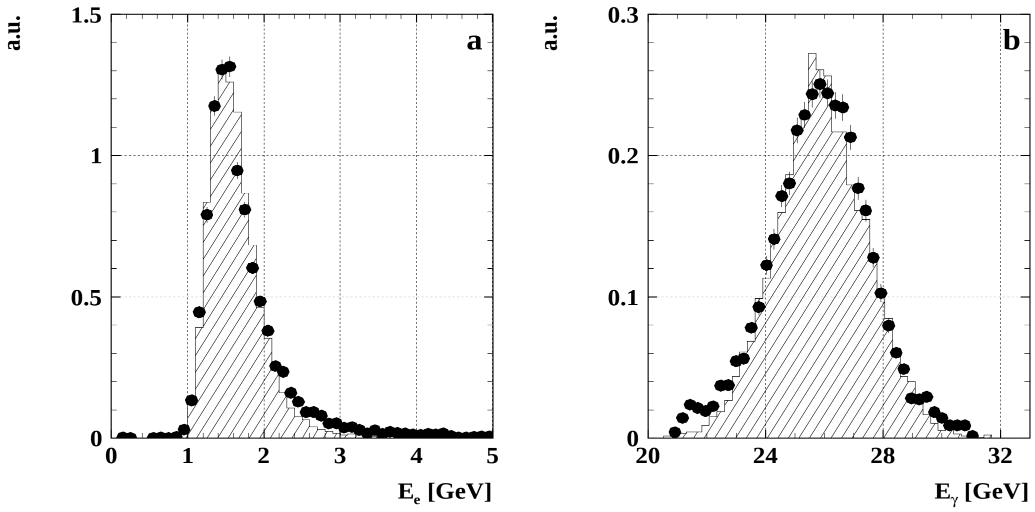

Figure 9: Comparison of the ET-8 data with Monte Carlo predictions first half of 1999 (electron case): the measured electron - (a) and photon - (b) energies gated by ET-8 for the bremsstrahlung events (symbols). The hatched histograms are MC calculation .

Fig.10 gives the same distributions but only for the positron case. It is clearly seen that the positron peak is shifted to 3 GeV and well separate from the trigger threshold compared to the electron case. The appropriated peak for the photons is shifted to the low energy direction and situated at 24.5 GeV.

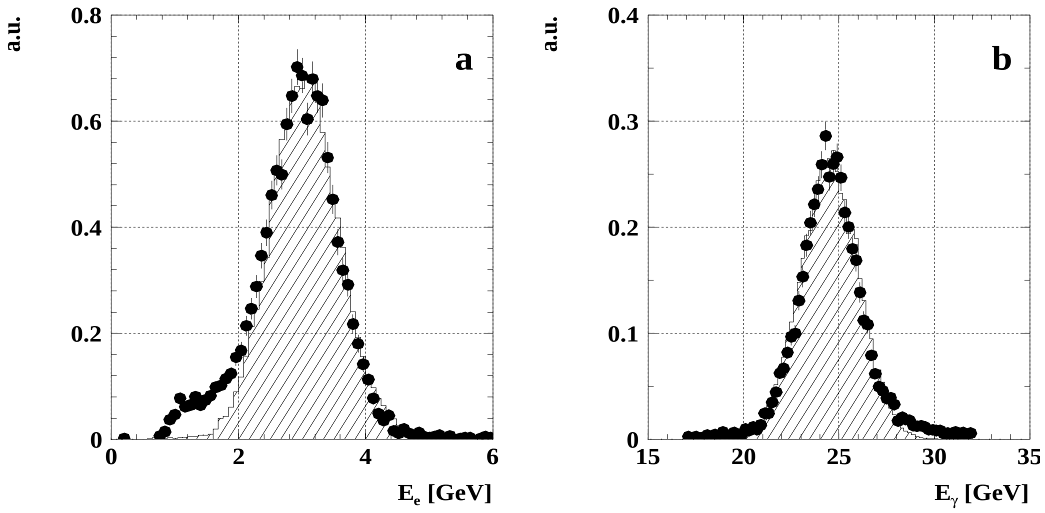

Figure 10: Comparison of the ET-8 data with Monte Carlo predictions second half of 1999 (positron case): the measured positron - (a) and photon - (b) energies gated by ET-8 for bremsstrahlung events (symbols). The hatched histograms are MC calculation .

The next step is to use the tuned X_{off} value to simulate the photoproduction events in the region $Q^2 < 0.01\ GeV^2$. The quality of the description of the photoproduction process by MC is illustrated in Fig.11 where the energy distribution of the accepted electrons for the photoproduction candidates (*"S82-subtrigger"*, special minimum bias run in 1999) is shown and compared to the MC calculation.

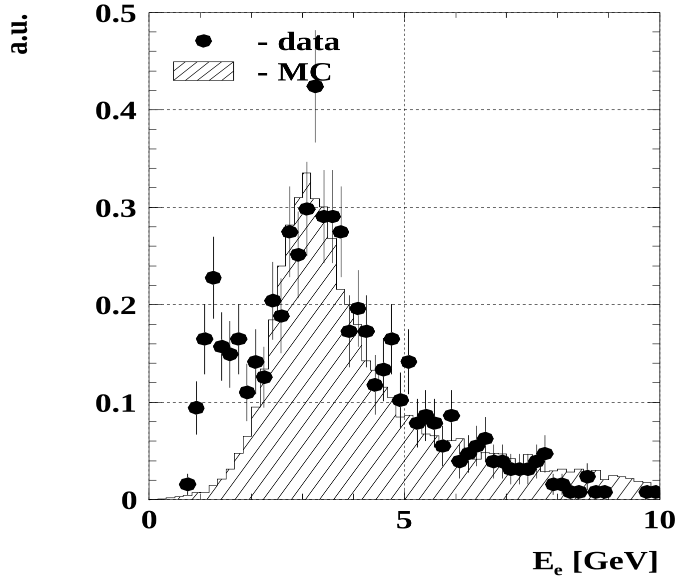

Figure 11: Energy distribution of the accepted by ET-8 tagger electrons for the photoproduction candidates: symbols - experimental data (*"S82-subtrigger"*) and hatched histogram - MC calculation.

The *"S82-subtrigger"* is formed by the following trigger elements conditions:
S82 = etag_8 & **DCRPh_T**$_c$ and globals **v:0 f:0 t:0**, where **etag_8 = LU_ET8** & **!LU_PD**.

The excess over MC at the low energy part of the distribution is maybe connected with the presence of background in this part of spectra. The source of this background is a random coincidence the electrons from bremsstrahlung not rejected by the anti-coincidence with the photon arm (the efficiency of the photon arm $\sim 95-98\%$) and the beam-gas interactions accepted by the main H1 detector. The value of this background could be large due to the low cross section of the photoproduction processes in this energy range compared to bremsstrahlung processes.

Using the parameters of the electron beam obtained in this way the acceptance of ET-8 for the photoproduction process as function of quasi-real photon energy is calculated. The information about acceptance behaviour and the trigger efficiency for the different sub-samples is written in the run dependent LET2 bank which is stored into the H1 database. The structure of this bank is shown below

```
!       BANKname BANKtype       ! Comments
!
        LET2                    ! ET-8 acceptance parametrization from MC
!
!   ATTributes:
!   -----------
! COL ATT-name FMT  Min   Max   ! Comments
!
   1  EFF0      F    0.    1.   ! Trigger efficiency
   2  YM        F    0.    1.   ! Trigger threshold value
   3  SIGY      F    0.    1.   ! Sigma of trigger threshold
   4  PVETO     F    0.    1.   ! Gamma-arm veto level
   5  YMIN      F    0.    1.   ! Minimum y-value
   6  YMAX      F    0.    1.   ! Maximum y-value
   7  DY        F    0.    1.   ! =0.005 y-step for parametrization
   8  Y1        F    0.    1.   !
  ...                           !
 N+8  YN        F    0.    1.   !
                                !
  END TABLE
```

The next Fig.12 shows the calculated acceptance functions for the different run periods for the first (electron case) and for the second (positron case) half of 1999.

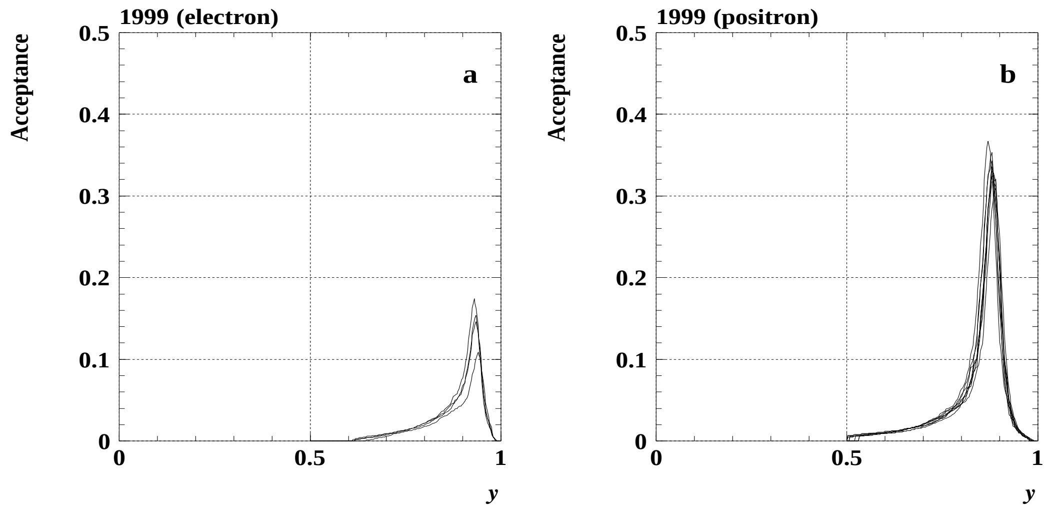

Figure 12: Calculated acceptance for the photoproduction process in 1999: a - electron case (first half of the year); b - positron case (second half of the year).

These acceptances are calculated using the new run dependent subroutine **ACET8(IRUN,Y,MODE)** which is now available in the H1UTIL library. This subroutine provides the acceptance for the different y-value for the photoproduction process. Parameter **MODE = 1** is used when the trigger effects (the trigger efficiency of ET8 trigger element and γ-arm veto condition) are applied.

The simulation of the ET-8 is not presently included in H1SIM and for this reason it is recommended to use this routine both for the analysis of the experimental data and for the Monte Carlo events. In order to describe correctly the acceptance effects every event should be used with the corresponding weight **W=ACET8(IRUN,Y,MODE)**. Where Y is a generated y-value $(1.-\mathrm{E}_{e'}/\mathrm{E}_e)$ from **GKI** bank for the MC and a measured electron energy $E_{e'}$ for the data. Finally this subroutine gives the possibility to restrict the y-range to more effectively use the MC statistics and analysis of the data.

5 Systematic error

The first source of the systematic error comes from the determination of the electron energy scale. The accuracy of the electron energy scale is connected with the photon energy through the calibration procedure. The precision of the photon energy scale at $\sim$ 25 GeV is about $\sim$ 0.42 % (or $\sim$ 100 MeV) resulting in an uncertainty in the electron energy scale of $\sim$ 3 GeV, about $\sim$ 3.5 %. Such energy uncertainty forces to $\sim$ 4.5 % error in the acceptance determination.

The ET-8 acceptance is strongly dependent on the position of electron tagger with respect to the electron beam. This position is known with precision of $\sim$0.5 mm which gives the uncertainty in the acceptance determination $\sim$ 4 %.

The error in the trigger efficiency determination gives about $\sim$ 1 % uncertainty in the acceptance.

And the last essential component to the acceptance uncertainty of ET-8 comes from the fitting procedure and the averaging of the calibrations samples and gives $\sim$ 1 % additional error to the acceptance determination.

So the overall systematic error in the acceptance determination of the ET-8 in 1999 could be taken as 6.2 %.

6 Conclusions

The electron tagger ET-8 was installed in 1998 and successful operated during this time.

The procedure of acceptance determination are developed and obtained results are stored in the new set of run dependent bank LET2 which is kept then in H1 database.

The total systematic uncertainty in the acceptance determination for the ET-8 electron calorimeter in 1999 is 6.2 %.

7 Acknowledgements

We gratefully acknowledge the support of the DESY directorate, directorate and machine group of the LPI synchrotron (Troitsk). Those of us from outside DESY wish to thank the DESY directorate for the kind hospitality extended to us. It is also a pleasure to thank P.Biddulph and R.Eichler for active support and helpful discussions. We would like to thank INTAS, RFBR (grant INTAS-RFBR 95-0679) and UK PRARC for financial support.

References

[1] H1 SpaCal group, Performance of an Electromagnetic Lead/Scintillating -fibre Calorimeter for the H1 Detector, DESY preprint, DESY-95-165.

[2] H.Bethe and W.Heitler,Proc. Roy. Soc. A146 (1934) 83.

[3] H1 Collab., Experimental Study of Hard Photon Radiation Processes at HERA, DESY Preprint, DESY-95-024.

[4] N.Gogitigze and S.Levonian, H1LUMI - An Offline Luminosity determination for the 1995 e^+ Data, H1 note, H1-0296-471 (1996).

[5] S.Levonian, H1LUMI - A Fast Simulation Package for the H1 Luminosity System, H1 note, H1-04/93-287 (1993).

[6] HERA Lattice and Optics Design, DESY HERA 92-07 (1992) 26.

[7] S.Levonian, Help for the e-tagger related analysis, http://www-h1.desy.de/ f11lev/QPETAC.html

[8] V.Andreev, Acceptance determination of electron tagger (ET44) in 1995, H1 note, H1-10/96-493.